Supporting Information

Unusual Sequential Annealing Effect in Achieving High Thermal Stability of Conductive Al-doped ZnO Nanofilms

Ruolin Yan,[1] Tsunaki Takahashi,[2,3*] Masaki Kanai,[1] Takuro Hosomi,[2,3] Guozhu Zhang,[1] Kazuki Nagashima,[1,3] and Takeshi Yanagida[1,2*]

[1] *Institute for Materials Chemistry and Engineering, Kyushu University, 6-1 Kasuga-Koen, Kasuga, Fukuoka 816-8580, Japan*
[2] *Department of Applied Chemistry, Graduate School of Engineering, The University of Tokyo, 7-3-1 Hongo, Bunkyo, Tokyo 113-8656, Japan*
[3] *JST, PRESTO, 4-1-8 Honcho, Kawaguchi, Saitama 332-0012, Japan*

Corresponding authors' e-mails:
takahashi-t@g.ecc.u-tokyo.ac.jp, yanagida@g.ecc.u-tokyo.ac.jp

Contents

Temporal Thermal Tolerance Tests of Sequentially Annealed AZO

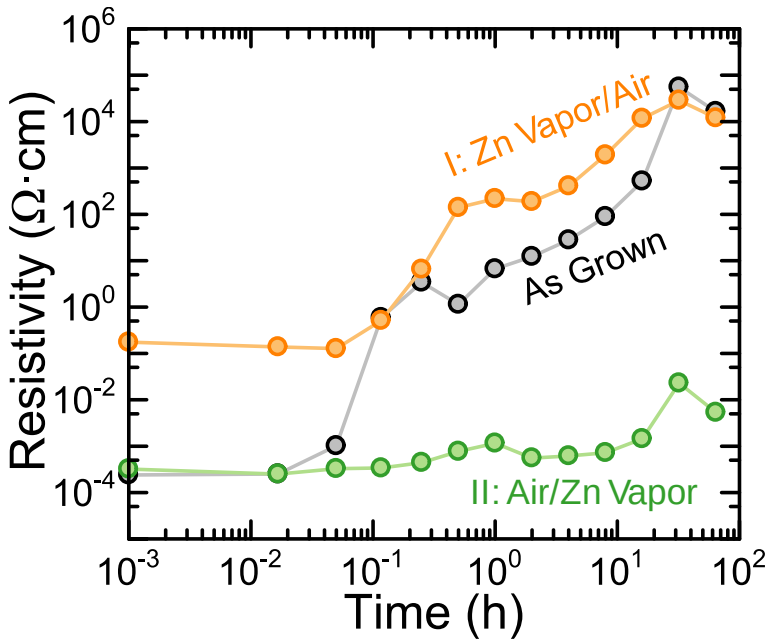

Figure S1. Thermal tolerance tests of resistivity of sequentially annealed AZO nanofilms at 400 °C for varied thermal stress time in ambient air. Test results of the as-grown AZO nanofilm are also shown for comparison. All resistivity measurements were performed at room temperature.

Morphology of AZO Nanofilms

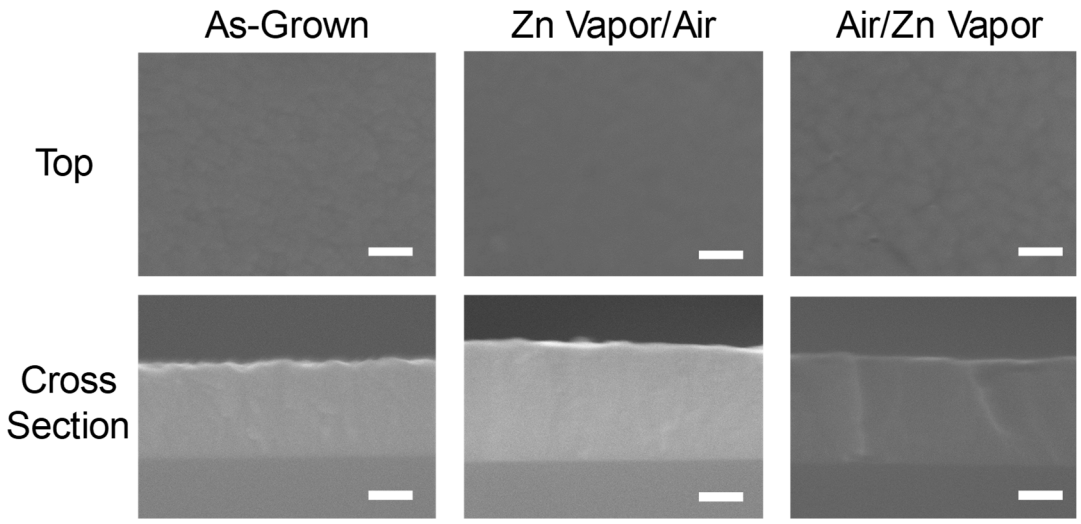

Figure S2. Field emission scanning electron microscopy (FESEM) images of as-grown and sequentially annealed AZO nanofilms.

PL Spectra of AZO Nanofilms after Thermal Tolerance Tests

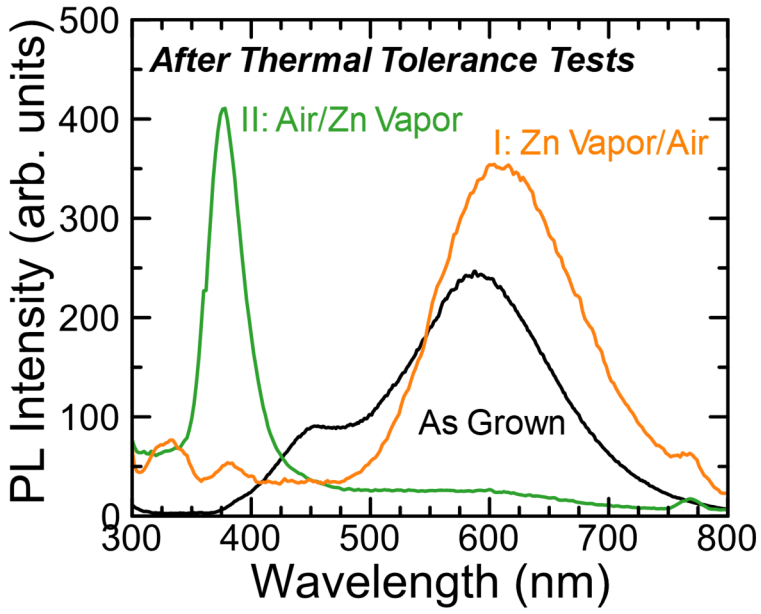

Figure S3. Photoluminescence (PL) spectrum of AZO nanofilms for Sequence I annealed, Sequence II annealed, and as-grown samples after the thermal load which is the same as total thermal loads of the thermal tolerance tests in Fig.2d. The single ultraviolet emission at approximately 380 nm of the Sequence II sample indicates that the low-defect structure of Sequence II AZO is maintained even after the thermal load. On the other hand, the as-grown AZO sample exhibits a broad luminescence around 600 nm similar to the Sequence I sample, indicating an increase in crystal perfections during the thermal load.

Sequential Annealing Effect

To explain the observed effect of annealing atmosphere sequence on the stability of ρ_{AZO} under atmospheric conditions, we assume that air annealing (oxygen-rich) and Zn vapor annealing (zinc-rich) mainly compensates an oxygen vacancy and a zinc vacancy, respectively. Based upon this assumption, we consider that the observed sequential effect of annealing atmospheres is equivalent to a sequential compensation of oxygen and zinc vacancies within AZO films. The point that we should explain here is why the different annealing sequence causes different results. When oxygen and zinc vacancies behave independently from each other within the AZO films, the sequential effect does not exist. Therefore, we must consider the correlation between the two different vacancies. A possible explanation is based on a deviation of a realizable formal ionic charge from its ideal value under an applied annealing atmosphere. In general, Al, Zn, and O ions have 3+, 2+, and 2- charges, and it is well-known that other valence charged states for these ions are unstable within ZnO. For simplicity, we assume that the formal charges are fixed for aluminum (Al^{3+}) and oxygen (O^{2-}), and the formal charge for zinc is determined by charge neutrality of the whole AZO system. Therefore, an *n*-type carrier in AZO is expressed by the deviation of the formal Zn charge from 2+ ($Zn^{+2-\delta}$). When Zn vapor annealing compensates only the cation vacancies in AZO, the *n*-carrier concentration must increase because of charge neutrality, and the formal charge of Zn decreases away from 2+ state. As-grown AZO, however, has a sufficient number of *n*-type carriers, and the Zn formal charge deviation from ideal 2+ is already substantial. Since such compensation drives the formal charge of Zn towards the unstable Zn+, a very high chemical potential of Zn (e.g., a high partial pressure of Zn vapor) is required. Achieving such a high chemical potential of Zn is difficult in the present annealing atmosphere, and as a result, Sequence I leaves a significant amount of cation vacancies during Zn vapor annealing. Conversely, air annealing for as-grown AZO to compensate the anion vacancies decreases the *n*-carrier concentration. This compensation is usually easy because this process drives the formal Zn charge towards the stable 2+ value. Since the formal charge of Zn in air-annealed samples is the stable 2+ state (Zn^{2+}), cation compensation to decrease formal charge (Zn vapor annealing) is easy compared to the compensation for as-grown AZO with a formal charge of $Zn^{+2-\delta}$. For this reason, only Sequence II can decrease both cation and anion vacancies.

Effects of Growth Temperature on Crystallinity of AZO

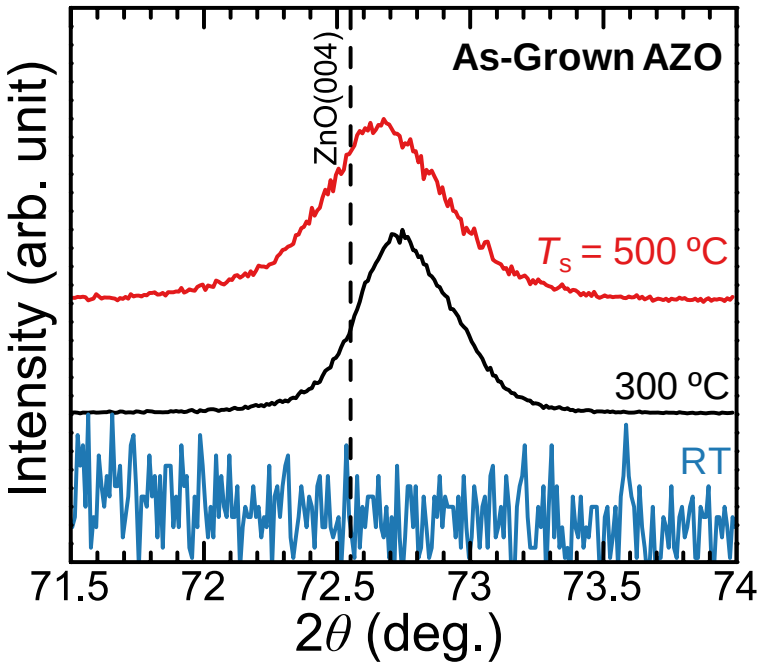

Figure S4. XRD patterns of as-grown AZO nanofilms for growth temperature (T_s) at room temperature, 300 °C, and 500 °C.

Benchmark of Conductivity of AZO

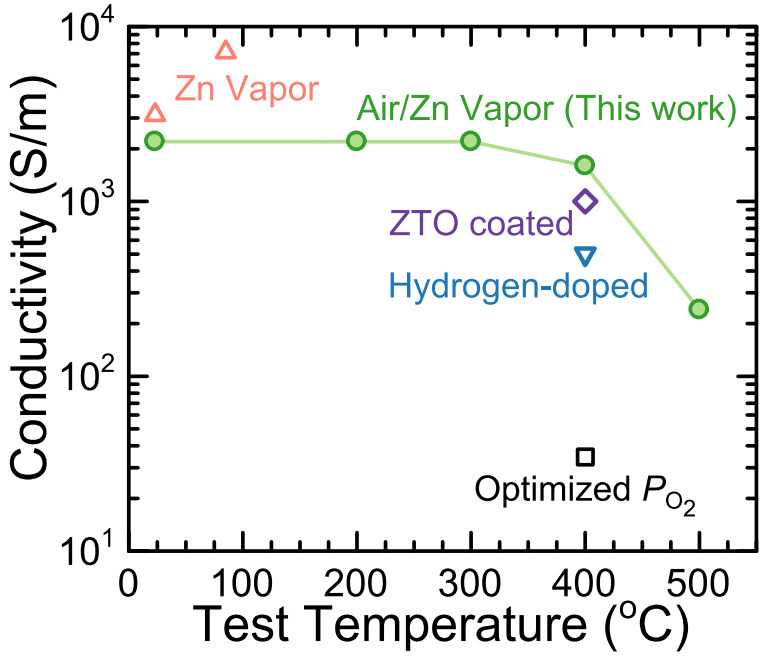

Figure S5. Thermal stress temperature dependence of electrical conductivities of AZO with various fabrication methods including Zn vapor annealing,[1-2] zinc tin oxide (ZTO) coating,[3] hydrogen doping,[4] optimization of oxygen pressure,[5] and Air/Zn vapor sequential annealing (this work). All electrical characterizations were performed at room temperature.

Sensor Properties of SnO_2 Nanochannel Sensor with Zn Vapor/Air Annealed AZO Electrodes

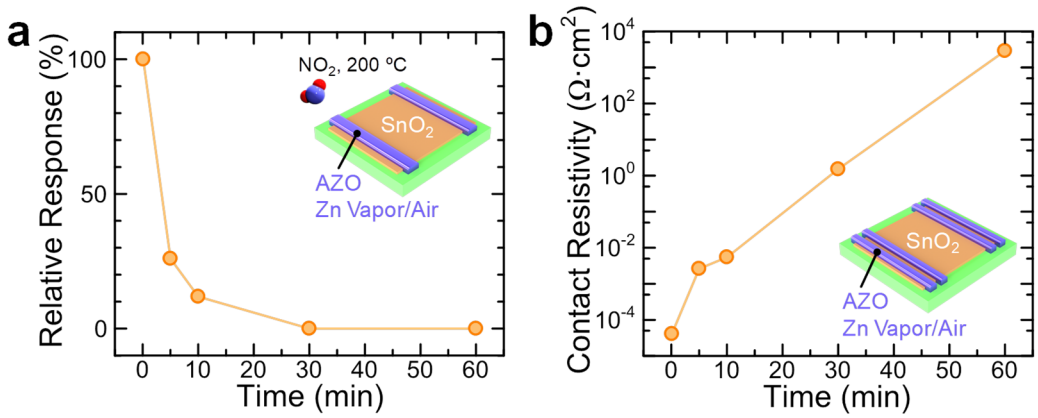

Figure S6. (a) Relationship between the relative sensor response to 100-ppm NO_2 and test duration (200 °C, ambient air) for SnO_2 nanochannel sensors with the electrodes of Sequence I (Zn Vapor/Air) annealed AZO nanofilms. (b) Relationship between contact resistivity and test duration (200 ºC, ambient air) for the SnO_2 nanochannel device with the four-terminal electrodes of Sequence I (Zn Vapor/Air) annealed AZO. The contact resistivity ρ_c is defined as $\rho_c = (R_2 - R_4)A_c$, where R_2, R_4, and A_c are two-probe resistance, four-probe resistance, and contact area on the nanochannel.

References

1. Hu, Q. C.; Ding, K.; Zhang, J. Y.; Yan, F. P.; Pan, D. M.; Huang, F.; Chiou, J. W. On the Variations of Optical Property and Electronic Structure in Heavily Al-doped ZnO Films During Double-step Growth Process. *Appl. Phys. Lett.* **2014,** *104*, 021913.
2. Zhan, Z.; Zhang, J.; Zheng, Q.; Pan, D.; Huang, J.; Huang, F.; Lin, Z. Strategy for Preparing Al-doped ZnO Thin Film with High Mobility and High Stability. *Cryst. Growth Des.* **2011,** *11*, 21-25.
3. Kim, I. H.; Ku, D. Y.; Ko, J. H.; Kim, D.; Lee, K. S.; Jeong, J. h.; Lee, T. S.; Cheong, B.; Baik, Y. J.; Kim, W. M. Improvement of the Thermal and Chemical Stability of Al Doped ZnO Films. *J. Electroceram.* **2006,** *17*, 241-245.
4. Lee, S.; Park, Y.; Kim, D.; Baek, D.; Yi, J.; Hong, B.; Choi, W.; Lee, J. Thermal Stability of Hydrogen-doped AZO Thin Films for Photovoltaic Applications. *Mater. Res. Bull.* **2014,** *58*, 126-131.
5. Bayraktaroglua, B.; Leedy, K.; Bedford, R. High Temperature Stability of Postgrowth Annealed Transparent and Conductive ZnO:Al Films. *Appl. Phys. Lett* **2008,** *93*, 022104.